RSC Advances

This is an *Accepted Manuscript*, which has been through the Royal Society of Chemistry peer review process and has been accepted for publication.

Accepted Manuscripts are published online shortly after acceptance, before technical editing, formatting and proof reading. Using this free service, authors can make their results available to the community, in citable form, before we publish the edited article. This *Accepted Manuscript* will be replaced by the edited, formatted and paginated article as soon as this is available.

You can find more information about *Accepted Manuscripts* in the Information for Authors.

Please note that technical editing may introduce minor changes to the text and/or graphics, which may alter content. The journal's standard Terms & Conditions and the Ethical guidelines still apply. In no event shall the Royal Society of Chemistry be held responsible for any errors or omissions in this *Accepted Manuscript* or any consequences arising from the use of any information it contains.

ROYAL SOCIETY OF CHEMISTRY

www.rsc.org/advances

Design, Synthesis and Biological Evaluation of Coumarin coupled nitroimidazoles as potential Imaging Agent

Nisha Saini, [†,‡] Raunak Varshney, [†] Anjani K. Tiwari, [#†] A.Kaul, [†] MPS Ishar, [‡] and Anil K. Mishra, [#†]

[†]Institute of Nuclear Medicine and Allied Sciences, Brig S K. Majumdar Road, Delhi-54, India

[‡]Department of Pharmaceutical Sciences, Guru Nanak Dev University, Amritsar-005, India

Corresponding Author #

Anjani K Tiwari & Anil K Mishra

Division of Cyclotron & Radiopharmaceutical sciences

Institue of Nuclear Medicine & Allied Sciences,Brig. Mazumdar Road,Timarpur

Delhi-110054

Email-anjani7797@rediffmail.com, Phone-91-11-23905387

Running Title- Coumarin coupled nitro-imidazole's in Cancer

Abstract- Solid tumors contain regions of hypoxia in comparison to normal tissues. The nitroimidazoles have shown great promise for targeting different type of cancers. The present work involves the design, syntheses, *in vitro* and *in vivo* investigation of hypoxia targeted nitroimidazoles radioconjugates (2NIHC and 4NIHC). Flow cytometry analysis showed that normoxic-hypoxic mean fluorescence of 2NIHC is 10 fold greater than of 4NIHC and much higher than the well-known pimonidazole hypoxia marker. Furthermore, molecular modeling studies of these ligands with CK2α revealed that 2NIHC is more potential CK2α inhibitor due to π-π interaction and H-Bonding with Val116, Glu114, Asp175, Asn161 and His160 in the active pockets of target. Radio labeling yield for both the complexes with ^{99m}Tc were >98%. Biodistribution in EAT tumor bearing mice demonstrated rapid clearance of ^{99m}Tc-2NIHC and high T/M ratio (3.57 %ID/g) as compared to ^{99m}Tc-4NIHC (2.05 %ID/g) at 4 hr. IC_{50} value of both ligands was estimated by MTS in different cell lines in addition to tumor regression study.

Key words- Imaging, Coumarin, Hypoxic, Flow cytometry and Nitroimidazole

RSC Advances Accepted Manuscript

ABBREVIATIONS

NIHC- Nitroimidazoles hydroxyl coumarin

NI- Nitroimidazoles

CK2- Casein kinase 2

EAT- Ehlrisch ascites tumor

GLIDE- Grid based ligand docking with energetic

MBq- Megabecquerel

PET- Positron emission tomography

XP- Extra precision

ITLC - Instant Thin Layer Chromatography

PAW- Pyridine, acetic acid and water

RSC Advances Accepted Manuscript

1. Introduction

Adaptation of tumor cells to hypoxia is a critical driving force in tumor progression and metastatsis (1). Such hypoxic zones have been postulated to have a reduced response to radiotherapy due to a decrease in oxygen free radicals. That are required to produce an enough DNA damage to give cell death (2). In addition, cells of these regions are considered to be chemo-therapy resistant due to limited delivery of drugs *via* circulation (3, 4). Therefore, identification of hypoxic zones becomes crucial for effective treatment of tumor.

A decade before assessment of hypoxia in tumor was difficult, as it involves the use of polarographic electrodes (5). It was invasive, expensive and limited for usage in few tumors. It led to the exploration of noninvasive method of diagnosing tumor hypoxia. In this regard, several probes have been developed to image hypoxia using PET and SPECT in nuclear medicine. Appropriately labeled nitroimidazoles (NI) are particularly attractive for imaging tumor hypoxia as nitro group undergoes one electron reduction by intracellular reductases, selectively in hypoxic conditions to generate reactive intermediates, which bind to cellular components and get trapped inside the cell (6). The PET radiotracer includes, [^{18}F] EF5 (7), [^{18}F] FETNIM (8), [^{18}F] FAZA (9) but the use of above markers get limited due to the choice of radioisotope and it has led to great interest in the development of ^{99m}Tc labeled compounds like BMS1813-21 (10), BRV59-21 (11)and HL91 (12-14).

A constraint in the development of radiopharmaceuticals is the inability to image at cellular and sub cellular level. Dual modality imaging is emerging as a method for improved visual quality as well as increase the qualitative accuracy of radio imaging for

RSC Advances Accepted Manuscript

diagnosis of a variety of diseases. For mechanistic studies of the uptake and bio-distribution in cells, the coupling of radio imaging with optical imaging is desirable. Chromophores are responsible for cell auto fluorescence predominantly in the blue region of the spectrum allowing the visualization at the cellular level. One of the used example is the nitro group which quenches the fluorescence of the ring system . Nitroimidazoles with fluorescent groups on side chain were well reported as hypoxic cell markers (15-16). We have selected substituted coumarins as fluorescent label for imaging hypoxic cells because substituted coumarins with electron donating group (-OH, $-OCH_3$) at 7^{th} position resulted in the increase of fluorescence (17-18).

Protein kinase CK2 often presents as a heterotetramer composed of two catalytic α subunits and two regulatory β subunits. Overexpressed CK2α is a key oncogenic force for tumorigenesis, and pharmacological inhibitors of this therapeutic target have been considered as promising drug candidates (19, 20). Besides that many hydroxycoumarins display IC_{50} (and Ki) values in submicro to nano level (17-18). Therefore here we report synthesis and biological evaluation of 7-hydroxycoumarin coupled nitroimidazole derivatives i.e. 2NIHC and 4NIHC.

2. Experimental Section

All the chemicals were purchased from Sigma-Aldrich and Merck. All solvents used were of analytical grades. TLC was run on silica gel coated aluminium sheets (Silica gel 60 F254, Merck, Germany) and visualized in UV light 254 nm. Radiocomplexation and radiochemical purity were checked by thin layer chromatography.

Instrumentation. ^{1}H and ^{13}CNMR spectra were recorded on a Bruker Avance II 400 MHz system (Ultra shield). Mass spectra (ESI-MS in positive and negative ion mode) were

RSC Advances Accepted Manuscript

performed on Agilent 6310 system ion trap. Radioimaging was performed using HAWKEYE gamma camera and single well type capintec γ scintillation counter respectively. Molecular modeling investigations were carried out using an advanced molecular docking program GLIDE, version 9.3 (Schrodinger, Inc, USA).

Cell culture.

Cells were maintained in Minimal Essential Medium supplemented with 10% fetal bovine serum, 4 mM glutamine, 1 mM sodium pyruvate, and 50 μg/mL gentamicin. Cells were grown in a humidified incubator at 37 °C/5% CO_2 and removed from flasks for passage or for transfer to 12-well assay plates by incubating them with 0.25% trypsin/EDTA.

Evaluation of *in vitro* specificity

Competion ability of the CA-IX inhibitor with ^{99m}Tc–2NIHC for binding to hypoxic HeLa cells was examined. HeLa cells were plated in 12-well plates at approximately 2.5 × 10^5 cells/well and allowed to adhere to the plate for 24 h. Cells were then incubated under hypoxic conditions (0.1% O_2/5% CO_2 at 37 °C) for an additional 24 h. The cells were then removed from hypoxia and incubated for 1 h in HBS Solution along with 0.5% BSA and 5nM ^{999m}Tc–2NIHC in the presence of 10 μM Actinomycin D. The assay media was then removed and the cells were washed 2× with cold HBS/0.5% BSA, collected by adding 0.25 mL of 1% SDS, and transferred to a 1.5 mL tube for counting the amount of radioactivity by gamma counter.

RSC Advances Accepted Manuscript

Flow Cytometric studies: - Cells of human lung carcinoma A549. 10^6 cells in 3 ml medium per petridish were cultured similarly as discussed above and maintained under normoxic condition (5% CO_2, 95% air) at 37^oC in a humidified CO_2 incubator. Cells were routinely subcultured twice a week using 0.05% of Trypsin (Sigma, USA) in 0.02% EDTA.

Animal Model. All animal experiments were done in accordance with the guidelines of Institutional animal ethics committee. EAT tumor bearing BALB/c mice were used for tumor regression study, biodistribution and gamma imaging. Mice were housed on normal diet of sterile food pellets and water at a controlled temperature of 22±2^oC.

BALB/c mice (aged 2 months) weighing between 20 and 25 g were selected for the study. EAT was maintained in the peritoneum of the mice in the ascites form by serial weekly passage. Exponentially growing EAT (Ehlrisch ascites tumor) cells were harvested, washed, and resuspended in PBS and 10^7 cells/mice were injected intramuscularly in the thigh of the left hind leg of the mice. Animal models were ready for hypoxic studies when tumor grew to a volume of 500-800 cm^3 in 12-14 days.

2.1 Synthesis

2.1.1 Synthesis of tert-butyl (2-amino-ethyl)-carbamate (2)

To a stirred solution of ethylenediamine 1 (3.0 ml, 45 mmol) in ethanol at 0^oC triethylamine (1.2 ml, 9.1 mmol) was added. The solution of boc-anhydride (2.0 g, 9.1 mmol) dissolved in 10 ml of ethanol was added dropwise after the reaction mixture was cooled down for 20 minutes. The reaction mixture was allowed to stir for 12 h and then solvent was evaporated to dryness under reduced pressure. The reaction mixture was

RSC Advances Accepted Manuscript

extracted with chloroform/water and combined organic extracts were dried over anhydrous sodium sulphate, evaporated under reduced pressure to obtain the transparent oily product (5.32 g, 79%). ^{1}H NMR (400MHz, $CDCl_3$) ^{1}H :- 1.45 (s, 9H, CH_3), 2.81 (t, 2H, J= 6.0 and 5.6 Hz, CH_2), 3.19 (t, 2H, J= 5.6 and 5.2 Hz, CH_2). ^{13}C NMR (100MHZ, $CDCl_3$) ^{13}C : - 28.37 (CH_3), 41.81, 43.29 (CH_2), 79.40, 156.2 (C=O). MS (ESI): found 161.2$[M+H]^+$,105.5 $[M- (C(CH_3)_3)]^+$.

2.1.2 Synthesis of tert-butyl{2-[7-hydroxy-2-oxo-2H-chromen-4-yl]-acetaamido}-ethyl-carbamte (4)

A solution of 7-hydroxy coumarinyl-4-acetic acid 3 (0.9 g, 4.5 mmol) and HOBT (0.61 g, 4.5 mmol) in dry DMF (25 ml) was stirred at 0^{o}C and a solution of DCC (1.0 g, 4.9 mmol) in dry DMF (5 ml) was added. Compound 2 (0.73 g, 4.5 mmol) was added at 0^{o}C to the reaction mixture and stirred for 2 h and then reaction mixture was stirred at rt for 24 h. The DCU (dicyclohrxylurea) was filtered off and solvent was concentrated under reduced pressure. The concentrate was dissolved in 1 ml of MeOH followed by addition of 30ml of cold chloroform dropwise. The compound gets precipitated out as pale white solid and purified by silica gel chromatography (20% methanol in chloroform with a yield of 1.35 g, 70%. ^{1}H NMR (400MHz, DMSO) ^{1}H :- 1.39 (s, 9H, CH_3), 2.83 (t, 2H, J= 6.0 and 6.0 Hz, CH_2), 3.07 (t, 2H, J= 6.4 and 5.6 Hz, CH_2). 3.76 (s, 2H, CH_2), 6.18 (s, 1H, CH), 6.72 (d, 1H, J=2.4 Hz, CH), 6.83 (dd , 1H, J_1=6.8 Hz, J_2=2.0 Hz, CH), 7.60 (d, 1H, J=8.4 Hz, CH). ^{13}C NMR (100MHz, DMSO) ^{13}C :- 27.34, 38.77, 39.44, 78.81, 102.24, 111.95, 112.28, 113.30, 127.20, 151.56, 155.45, 156.10, 160.73, 161.62, 168.21, 168.30. MS (ESI): found 362.1 $[M-H]^-$.

RSC Advances Accepted Manuscript

2.1.3 Synthesis of N-(2-Amino-ethyl)-2-(7-hydroxy-2-oxo-2H-chromen-4-yl)-acetamide (5)

The *tert*-butyl group of compound 4 (1.0 g, 2.7 mmol) was deprotected by the solution of trifluoroacetic acid (5 ml) in anhydrous dichloromethane at 0^{o}C and followed by stirring at room temperature for 6 hr. The solvent was evaporated to dryness under reduced pressure to obtain the crude product. The product was washed with methanol (3×20 ml). Addition of cold diethyl ether led to the precipitation of pure product as white solid (0.66 g, 69% yield). ^{1}H NMR (400MHz, D_2O) ^{1}H: - 3.01 (t, 2H, J= 4.0 and 8.0 Hz, CH_2), 3.40 (t, 2H, J= 4.0 and 8.0 Hz, CH_2)., 3.72 (s, 2H, CH_2), 6.11 (s, 1H), 6.64 (s, H, CH), 6.74 (d, 1H, J=8.0 Hz, CH), 7.40 (d, 1H, J=8.0 Hz, CH). ^{13}C NMR (100MHz, D_2O) ^{13}C :- 37.04, 38.47, 38.88, 102.80, 112.02, 112.05, 113.58, 126.22, 151.34, 154.51, 160.07, 164.03, 172.04. MS (ESI): found 261.1 $[M-H]^-$; 175.1 $[M-CH2CONH(CH_2)_2NH_2]^-$.

2.1.4 Synthesis of 1-(4-Bromo-butyl)-4(or 2)-nitro-1H-imidazole (8, 9)

A solution of 4-nitroimidazole and 2-nitroimidazole (1.0 g, 8.9 mmol) and K_2CO_3 (9.8 g, 71.3 mmol) in MeCN (50 ml) was stirred at 70^{o}C for 0.5 hr followed by the addition of 1, 4-dibromobutane (4.2 ml, 35.7 mmol). After completion, reaction mixture was filtered, evaporated under reduced pressure and purified by silica gel chromatography (10% methanol in chloroform). The product was crystallized as pale yellow crystal of 4-nitroimidazole derivative (1.22 g, 76% yield) and yellow powder of 2-nitroimidazole derivative (1.31 g, 79% yield) in hexane.

4-nitroimidazole derivative: - ^{1}H NMR (400MHz, D_2O) ^{1}H: 1.83-1.96 (m, 2H), 1.99-2.10 (m, 2H), 3.42 (t, J= 6.0 and 6.0 Hz, 2H), 4.09 (t, 2H, J= 7.2 and 7.2 Hz). 7.53 (s, 1H),

RSC Advances Accepted Manuscript

7.85 (s, 1H). ^{13}C NMR (100MHz, D_2O) ppm: 29.15, 32.29, 47.60, 119.35, 136.06, 148.11. MS (ESI): found 248.0 and 250.0 $[M+H]^+$, 270.0 and 272.2 $[M+Na]^+$ with isotopic pattern of Br.

2-nitroimidazole derivative: - ^1H NMR (400MHz, D_2O) ^1H: 1.89-1.96 (m, 2H), 2.01-2.14 (m, 2H), 3.41 (t, J= 6.4 and 6.4 Hz, 2H), 4.45 (t, 2H, J= 7.2 and 7.2 Hz). 7.13 (d, 2H, J=6.0 Hz). ^{13}C NMR (100MHz, D_2O, Me4Si): ^{13}C = 29.29, 30.93, 32.38, 49.43, 126.02, 128.52. MS (ESI): found 248 and 250 $[M+H]^+$ with isotopic pattern of Br.

2.1.5 Synthesis of 2-(7-Hydroxy-2-oxo-2H-chromen-4-yl)-N-{2-[4(or2)-nitro-1H-imidazole-1-yl)-butyl)amino]-ethyl}-acetamide (10 (2NIHC), 11(4NIHC))

Triethylamine (0.15 ml, 1.14 mmol) was added to the stirred solution of 5 (0.2 g, 0.76 mmol) in water. It was allowed to stir for 15 min followed by the addition of 8 (0.18 g, 0.76 mmol) and heated to 80^{o}C. Reaction was continued for 10 hr and the progress of the reaction was monitored by TLC. Reaction mixture was evaporated under reduced pressure, dissolved in minimum amount of methanol and get precipitated as light brown solid with the addition of cold diethyl ether. Yield of 2-nitroimidazole derivative (2NIHC) and of 4-nitroimidazole derivative (4NIHC) was (0.24 g, 68% yield), (0.19 g, 60% yield) respectively.

2-nitroimidazole derivative: - ^1H NMR (400MHz, DMSO) ^1H : 1.73-1.79 (m, 4H, CH_2), 3.0 (brs, 4H, CH_2), 3.44 (brs, 4H, CH_2), 3.63 (s, 2H, CH_2), 4.27-4.34 (m, 2H, CH_2), 6.01 (s, 1H, CH), 6.35 (brs, 1H, CH), 6.60 (brs, 1H, CH), 7.00 (brs, 1H, CH), 7.29 (d, 2H, J=16.4 Hz, CH). ^{13}C NMR (100MHz, DMSO) ^{13}C : 26.22, 28.21, 37.13, 39.01, 49.90,

RSC Advances Accepted Manuscript

52.69, 60.99, 102.66, 111.81, 113.68, 126.30, 127.76, 127.94, 144.18, 151.31, 154.18, 160.35, 161.66, 163.69, 171.70. HRMS: 429.1782

4-nitroimidazole derivative: - ^{1}H NMR (400MHz, DMSO) ^{1}H : 1.69-1.76 (m, 2H, CH_2), 1.90-1.97 (m, 2H, CH_2), 2.39 (s, 2H,CH_2), 2.50-2.51 (m, 4H, CH_2), 4.10 (t, J= 6.4 and 6.4 Hz, 2H, CH_2), 4.15 (t, J= 7.2 and 7.2 Hz, 2H, CH_2), 6.20 (s, 1H, J=0.8 Hz, CH), 6.71 (br, s, NH), 6.93- 6.96 (m, 2H, CH), 7.35 (br, s, 1H, NH), 7.67 (d, 1H, J=8.8 Hz, CH), 7.91 (dd, 1H, J= J= 10.8 and 10.8 Hz, Hz, CH), 8.46 (dd, 1H, 10.4 and 10.4 Hz, CH). ^{13}C NMR (100MHz, DMSO) ^{13}C : 18.59, 22.91, 25.68, 27.13, 47.50, 68.02, 101.62, 111.53, 112.95, 113.55, 122.03, 126.94, 137.90, 147.41, 154.01, 155.16, 162.02, 172.24. HRMS: 429.1846

2.2 *In-vitro* Study

2.2.1 Cell uptake by Flow Cytometry

To evaluate cell uptake, exposure of hypoxia was given to A549 cell line (<1% O_2) in a hypoxic chamber. Hypoxic and normoxic A549 cells were incubated with 2NIHC and 4NIHC for 4h at different concentration of 10mM, 10μM and 10nm. After incubation cells were washed with PBS twice, detached using a treatment of 0.5 ml of trypsin for 5 minutes and resuspended in PBS. 6 μl of 1 μg/ml of propidium iodide in PBS was added, incubated for 30 min in the dark at -4 °C and then samples were analyzed by flow cytometry with a Flow cytometer FACS calibur.

2.3 Computational Analysis

2.3.1 Receptor for Docking

Over actvation of receptor protein kinase CK2α is a key factor in tumor genesis. Thus there is increasing interest on the deactivation of CK2α to inhibit the growth of cancerous

RSC Advances Accepted Manuscript

cells. The human CK2 catalytic subunit was built using a homology modeling approach with α isoform as template (PDB code ID: 2ZJW). In order to gain insight into the putative binding mode of the 2NIHC with CK2α it is docked with a crystallographic structure of CK2α.

2.3.2 Ligand-Receptor Docking

X-ray crystal structure of human protein kinase CK2α complexed with ellagic acid [PDB ID: 2ZJW] with resolution of 2.40 A^o) was taken for molecular docking studies. The following criteria were kept in mind before choosing the protein- ligand complexes: non-covalent binding between protein and ligand, crystallographic resolution less than or equal to 3A^o and known experimental binding data. During the docking process, initially GLIDE performs a complete systematic search of the conformational, orientation and positional space of the docked ligand and eliminating unwanted conformations using scoring and followed by energy optimization. Preparation of the protein for docking included removal of unnecessary heteroatom and solvent coupled with addition of hydrogen atoms, bond order for crystal ligand and protein were adjusted and minimized up to 0.30A^o RMSD. Using extra precision (XP) mode of GLIDE application, docking studies was performed on coumarin derivative. Using 'Glide grid generation' the binding region was defined by a 36.75Å, 4.62Å, and 9.61Å box centred on the centroid of the crystallographic ligand to confine the centroid of the docked ligand. No scaling factors were applied to the Vander Waals radii. Best pose was selected on the basis of Glide score and the interactions formed between the ligands and active site amino acids.

Docking experiments were carried out by using GLIDE (grid based ligand docking with energetic) and ligand docking programme from calculations in extra precision (XP)

RSC Advances Accepted Manuscript

mode. The docking was initiated with putting specified receptor grid and prepared ligand molecule together. GLIDE was run in the flexible docking mode which automatically generates conformations for each input ligand. The combination of position and orientation of a ligand relative to the receptor, along with its conformations in flexible docking is referred to as a ligand pose. The ligand poses that GLIDE generates pass through a series of hierarchial filters that evaluate the ligand's interaction with the receptor. The initial filters test the spatial fit of the ligand to the defined active site, and examine the complentarity of ligand-receptor interactions using a grid based method pattern after the empirical chemscore function. Poses that pass their initial screens enter the final stage of the algorithm, which involves evaluation and minimization of a grid approximation to the OPLS-AA non-bonded ligand receptor interaction energy. Final scoring was then carried out on the energy minimized poses. By default, Schrodinger's proprietary Glide Score multi-ligand scoring function was used to score the poses and analyze the result of binding affinity on the basis of the score. The time to dock one ligand was approximately 2-5 min.

2.4 Radiochemistry

2.4.1 ^{99m}Tc Radiocomplexation of 2-NIHC and 4-NIHC. The ligand i.e. 2-NIHC and 4NIHC (4.6 mmol) was dissolved in 1ml of double distilled water. 100 μL of this solution was taken in sealed glass vial and stannous chloride (1 μmol; 1 mg) dissolved in 1ml of 10% acetic acid purged with N_2) was added to it followed by the addition of freshly eluted ^{99m}Technecium pertechnetate (2 mCi; 200μl) saline solution. The pH of the reaction mixture was adjusted to 7 using 0.1 M sodium carbonate solution. All contents were thoroughly mixed and vial was kept at room temperature for 0.5 h.

RSC Advances Accepted Manuscript

2.4.2 Radiochemical purity of ^{99m}Tc-2NIHC and 4-NIHC complex

The radiolabeling efficiency of above complexes was determined by using ascending instant thin layer chromatography on ITLC-SG (Paul Gelman, USA) using solvents 100% acetone, pyridine/acetic acid/water (PAW) (3:5:1.5) and saline. TLC strips were cut into 0.5 cm fragments and counts of each fragment were taken. The complexed ^{99m}Tc remained at the origin whereas free ^{99m}Tc moved with the solvent front.

2.4.3 Serum stability of complex

To measure the stability of the labeled complex, human serum was incubated with ^{99m}Tc radiolabeled complex at 37^{o}C for 1 h in a humidified incubator maintained at 5% CO_2 and 95% air. Samples were centrifuged and serum was filtered through 0.22µm syringe filter into a sterile plastic culture tubes. The radiolabeled conjugate was immediately placed in a CO_2 chamber incubated at 37°C and then analyzed for any dissociation of the complex by ITLC strips with 100% acetone and pyridine, acetic acid and water (PAW) (3:5:1.5) as a mobile phase. Percentage of free pertechnetate at different time intervals was estimated from it, which gives the percentage labeling efficiency or dissociation of the complex.

2.5 In-vivo Study

2.5.1 Biodistribution Study in mice bearing hypoxic tumor

This study was done after 12 days of inoculation of EAT cells into BALB/c mice, so that hypoxic conditions were generated in tumor for its assessment. Approximately 2 mCi of ^{99m}Tc-2NIHC and ^{99m}Tc-4NIHC was injected intravenously into tumor bearing BALB/c mice through tail veins. At 1hr, 4h and 24h post injection, mice were sacrificed by cervical dislocation. Biodistribution measurements were evaluated in tumor and in

RSC Advances Accepted Manuscript

various organs including lung, liver, kidney, stomach, blood and muscle. The selected tissues and organs were harvested and weighed. Uptake of ^{99m}Tc radioactivity in each sample was measured as %ID/g of the tissue with an automated gamma scintillation counter and was normalized with ^{99m}Tc-decay correction.

2.5.2 Scintigraphy in mice bearing normal and hypoxic tumor

As it was cleared from the biodistribution studies that 2NIHC accumulates more in the hypoxic tumor than 4NIHC along with fast clearance from the body. Therefore scintigraphic imaging of mice bearing hypoxic tumor was done with only 2NIHC. After intravenous injection of 2 mCi of ^{99m}Tc-2NIHC in mice bearing hypoxic tumor, animals were subjected to SPECT imaging at different time intervals of 1, 4 and 24 h post injection with an acquisition time of 10 min/view. The effect of ^{99m}Tc-2NIHC and ^{99m}Tc-4NIHC was also observed in normal tumor bearing mice where tumor was ~1 week old. Image acquired at 4 h post injection shown the maximum drug uptake in hypoxic tumor site and at same time also taken for normal tumor bearing mice. The regions of interest (ROI) were drawn on the right thigh at tumor site and to the contralateral muscle indicating specific and non specific binding of drug. The tumor to muscle ratio was calculated from the counts per pixel of the ROI.

2.5.3 Antitumor Screening

7-Hydroxy coumarin and its derivatives were selective inhibitor of tumor growth, to evaluate the effect of pharmacological inhibition of tumor growth in vivo, we treated mice bearing EAT tumor only with 2NIHC. As molecular docking studies have shown that 2NIHC is more potent anticancerous drug than 4NIHC. Animals were randomly divided into three groups (control, 2NIHC dose 1 and dose 2) with each group having

RSC Advances Accepted Manuscript

three mice. After initial implantation of cells, tumors were allowed to grow for 3 weeks till they become hypoxic and then treatment was initiated. In one set of group (n=3), 2NIHC (1mg/ml) was administered on the 15th day of implantation of tumor by intravenous injection via a lateral tail vein at a dose of 5mg/kg to one group and other group as 30mg/kg. Another set was taken as control which was without any vehicle. The dosing schedule involved injections every alternate day for doses 2 and 3 i.e. on 17th and 19th, followed by injection every third day i.e. 23rd and 27th day for remaining doses . Tumor diameters were measured on days 17, 19, 23, 27 and 31 with digital calipers and tumor volume was measured using the modified ellipsoid formula ($LxW^2/2$). Throughout the experiments, all animals were accommodated in a pathogen-free laboratory environment. The study was terminated at 30 days post treatments.

3. Results and discussion

3.1 Chemistry: Synthesis of 7-hydroxycoumarin coupled 2(4)-nitroimidazole derivatives.

The mono *tert*-butyl ester of ethylenediamine was achieved by the controlling the stoicmetric amount of boc-anhydride. The (2-Amino-ethyl)-carbamic acid *tert*-butyl ester 2 was prepared by dropwise addition of boc-anhydride to ethylene diamine in the presence of triethylamine at 0^{o}C followed by stirring at room temperature for 12 h in good yield (79%) (Scheme-1).The oily product was obtained used as such without further purification. The COOH group of 7-hydroxy coumarinyl-4-acetic acid 3 was in situ converted into to the active ester by using HOBT and DCC in dried DMF. The active ester was coupled to the NH_2 group of synthesized oily compound for 2 h at 0^{o}C. The

RSC Advances Accepted Manuscript

stirring was continued for 24 h at room temperature. The dicyclohexyl urea was filtered off and solvent was concentrated to afford the {2-[2-hydroxy-2-oxo-2H-chromen-4-yl)-acetylamino]-ethyl}-carbamic acid *tert*-butyl ester. The compound was purified by column chromatography to give 4 in 70% yield. Deprotection of *tert*-butyl ester 4 with trifluroacetic acid in dried DCM furnished N-(2-amino-ethyl)-2-(7-hydroxy-2-oxo-2-2H-chromen-4-yl)-acetamide 5 (69%) in 6 h. Additionally 2-nitroimidazole and 4-nitroimidazole were refluxed with 1,4-dibromobutane in the presence of potassium carbonate at 70^{o}C for 0.5 h. The reaction mixture was cooled down to the room temperature and K_2CO_3 was removed by simple filteration by Whatman filter paper. The compound was purified by column chromatography and finally crystallized to yielded 1-(4-Bromo-butyl)-4-nitro-1*H*-imidazole 8 as yellow powder and 1-(4-Bromo-butyl)-2-nitro-1H-imidazole 9 as yellow crystal respectively in 76-79% overall yields. The bromo group of nitoimidazole derivative 8 and 9 were finally reacted with substituted acetamide 5 at 80^{o}C for 10 h in presence of triethylamine to give the desired products i.e. 2-(7-hydroxy-2-oxo-2H-chromen-4-yl)-N-{2-[4-nitro-imidazole-1-yl)-pentylamino]-ethyl}-acetamide (4-NIHC) 10 and 2-(7-hydroxy-2-oxo-2H-chromen-4-yl)-N-{2-[5-(2-nitro-imidazol-1-yl)-pentylamino]-ethyl}-acetamide (2-NIHC) 11 in 60-68% yields.

Scheme 1. Synthesis of {2-(7-Hydroxy-2-oxo-2H-chromen-4-yl)-N-{2-[4(or2)-nitro-imidazole-1-yl)-pentylamino]-ethyl}-acetamide.

RSC Advances Accepted Manuscript

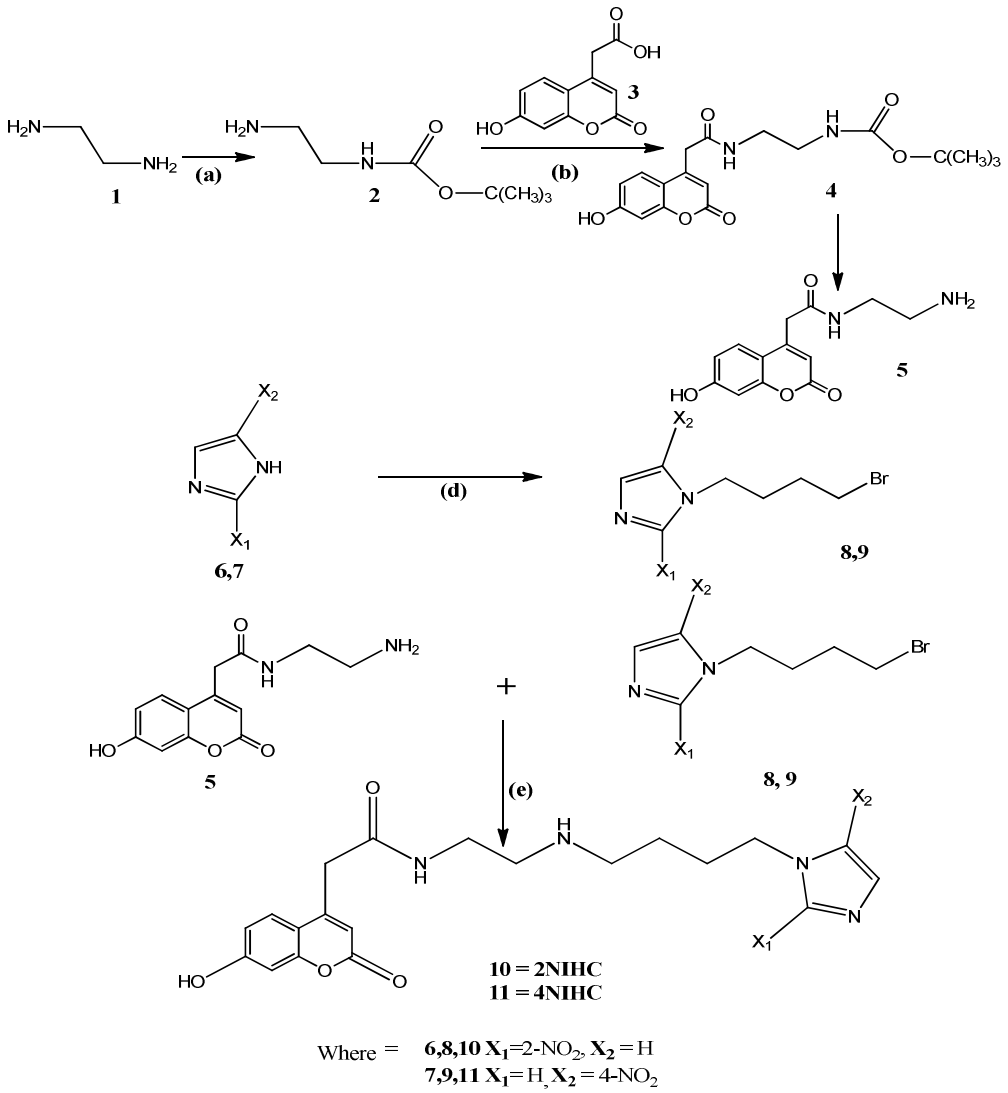

(a) $(boc)_2O$, TEA, 0°C–rt, 79%; (b) 7-hydroxycoumarinyl-4-acetic acid, HOBT, DCC, 70%; (c) TFA, 0°C, 69%; (d) 1,4-dibromobutane, K_2CO_3, 70°C, 76-79%; (e) TEA , 70°C, N-(2-Amino-ethyl)-2-(7-hydroxy-2-oxo-2-2H-chromen-4-yl)-acetamide, 60-68%.

3.2 Biological Characterization

3.2.1 In Vitro Binding

Before proceeding for their evaluation as a hypoxia marker, fluorescent spectra of 2NIHC and 4NIHC determined from a spectrofluorometer are illustrated in Figure 1 which

RSC Advances Accepted Manuscript

indicates that the both fluorescent coumarins have peak of emission wavelengths at 460 nm but the fluorescent intensity of 2NIHC is more than 4NIHC which makes 4NIHC more suitable for flow cytometric studies.

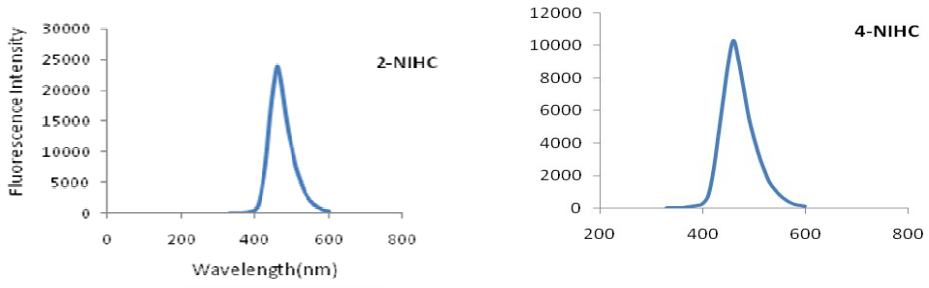

Figure 1. Fluorescence spectra measured by spectrofluorometer for 2NIHC and 4NIHC.

In vitro potency of 2NIHC and 4-NIHC was determined by flow cytometric analysis of cells incubated with both compounds under normoxic and hypoxic conditions as shown in Figure 2.

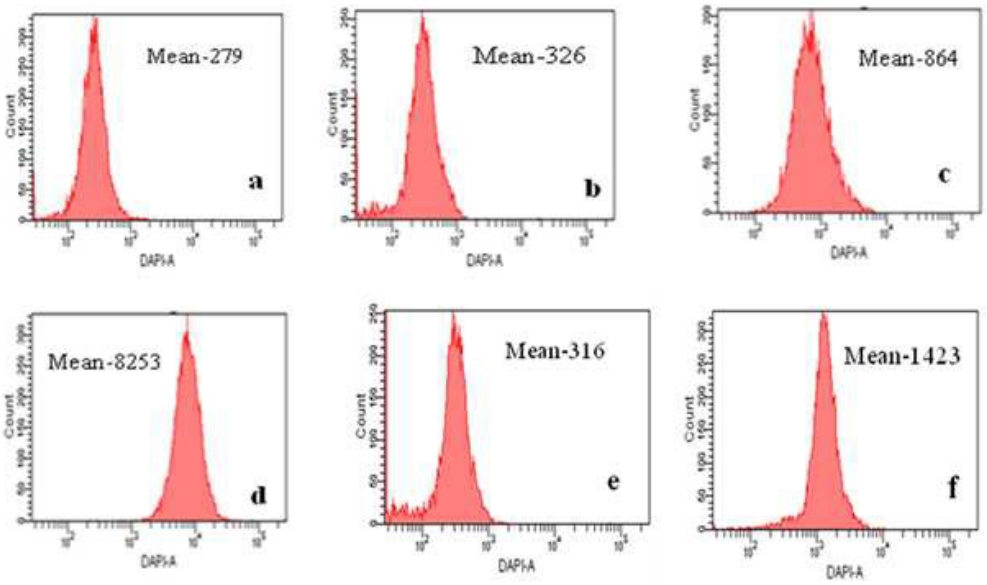

RSC Advances Accepted Manuscript

Figure 2. Flow cytometric analysis of A549 cells incubated at 37^{o}C with 10 mM of 2NIHC and 4NIHC for 4 h (a) control–hypoxic (b) control-oxic (c) 2NIHC-normoxic (d) 2NIHC-hypoxic (e) 4NIHC-normoxic (f) 4NIHC-hypoxic.

There was no significant difference in the controls of hypoxic and normoxic conditions and histograms of 2NIHC and 4NIHC can be compared to them. There was approximately 10 fold increase in mean fluorescence in hypoxic cells when A549 (21,22) cells were incubated with 2NIHC as compared to normoxic condition i.e from 864 to 8253. However in 4NIHC, only five time increase in uptake was noticed in hypoxic condition i.e 316 to 1423. The negligible amount of overlap between the fluorescence of hypoxic and well oxygenated cells incubated with 2NIHC would be a desirable property of a compound to measure a low proportion of hypoxic cells in a well oxygenated tumor. Mean fluorescence of pimonidazole (23) in normoxic as well as in hypoxic cell is 56.8 and 286 with cells in the range of 10^{1}-10^{3} i.e mean fluorescence increases only five fold in hypoxic cells. Comparative studies showed that mean fluorescence is much higher for 2NIHC with cells in the range of more than 10^{4}, which makes it a highly selective hypoxia marker.

The concentration dependent development of fluorescence in cells incubated with 2NIHC is shown in Figure 3. A large differential can be seen in fluorescence of cells incubated under normoxic and hypoxic conditions at different concentrations. Thus maximum fluorescence intensity was observed with 10 mM concentration of 2NIHC which indicates that drug binds firmly to the cellular macromolecules.

RSC Advances Accepted Manuscript

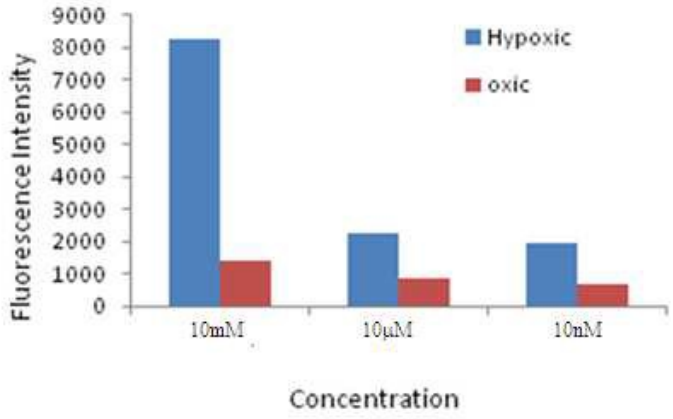

Figure 3. Mean fluorescence intensity from hypoxic and normoxic cells incubated for 4 h at 37^{o}C with 2NIHC.

3.2.2 Cytotoxicity assays

The cytotoxicity of compounds 2NIHC and 4NIHC was evaluated in vitro against human cervical carcinoma (HeLa) and human lung cancer (A-549) cell lines (Table I). As a screening assay, the cytotoxicity was tested using an MTS tetrazolium reduction assay, for HeLa cell lines, and expressed as IC_{50} values. IC_{50} is the concentration (μM) required to reduce the absorbance values, i.e., the capability of the cells to reduce MTS, by 50% after 24 h of treatment. In vitro growth inhibitory effect of these compounds on EAT cells was also determined by measuring the absorbance by same assay for living cells. Briefly, EAT cells were seeded in 96-well microtiter plates. After incubation for 24 h in a dose-dependent way for various time periods (0–24 h), 50 μL of solution (2 mg/mL in PBS) was added to each well, and plates were incubated for an additional 4 h at 37 °C and finally measuring the absorbance at 490 nm.

RSC Advances Accepted Manuscript

Determination of CK2α activity

The final reaction mixture (final volume of 40 µL) for the determination of CK2 activity (apoenzyme CK2α or holoenzyme CK2α/2β2) contained: casein substrate (75 µg) or peptide substrate (RRRDDDSDDD, 20 µM), Tris–HCl pH 7.5 (20 mM), $MgCl_2$ (20 mM) and appropriate concentrations of inhibitor in 1 µL DMSO. After 30 min of incubation at 30 °C, 40 µL of the assay mixture was spotted onto a square (2 cm × 2 cm) of Whatman 3 MM (for casein), which was immediately immersed in cold 5% (w/v) trichloroacetic acid containing 0.3% *o*-phosphoric acid (10 mL per square), and washed with H_2O three times for 10 min. Then the requisite squares were washed in 96% ethanol and dried. The radioactivity was quantified by liquid scintillation counter.

Table I. IC_{50} of nitroimidazoles

Compound	IC_{50} ± SD (µM)			
	HeLa	A549	EAT	CK2α
2NIHC	13.22 ± 0.95	9.58 ± 0.76	16.24 ± 0.42	11.28 ± 3.86
4NIHC	19.02 ± 1.02	15.78± 0.58	19.98± 0.17	27.18± 5.39
Actinomycin D	1.85 ± 0.46	1.16 ± 0.82	2.92 ± 0.66	4.86 ± 1.15
Doxorubicin	9.21 ± 0.32	6.08 ± 0.14	7.83 ± 0.82	6.32 ± 0.20

a-Cells were exposed in optimal culture conditions in 96-well plates to seven concentrations of the compounds (1, 5, 10, 15, 20, 25 and 100 µM) or control medium for 24 h before determining cellular metabolic activity by an MTS tetrazolium compound bioreduction assay.

b - Each value is determined from five samples using a non-linear regression analysis.

RSC Advances Accepted Manuscript

3.2.3- In vitro binding and selectivity

To ensure that the binding of ^{99m}Tc–2NIHC on HeLa cells was specific, cells were incubated with 5 nM ^{99m}Tc–2NIHC alone or in the presence of 10 μM Actinomycin D, after exposure of the cells to hypoxic or normoxic conditions for 24 h. As shown in Figure 4, ^{99m}Tc-2NIHC bound only to hypoxic HeLa cells and not to HeLa cells that remained under normoxic conditions. Further, the binding of ^{99m}Tc–2NIHC to the hypoxic HeLa cells was homogenised by coincubation with 10 μM Actinomycin D.

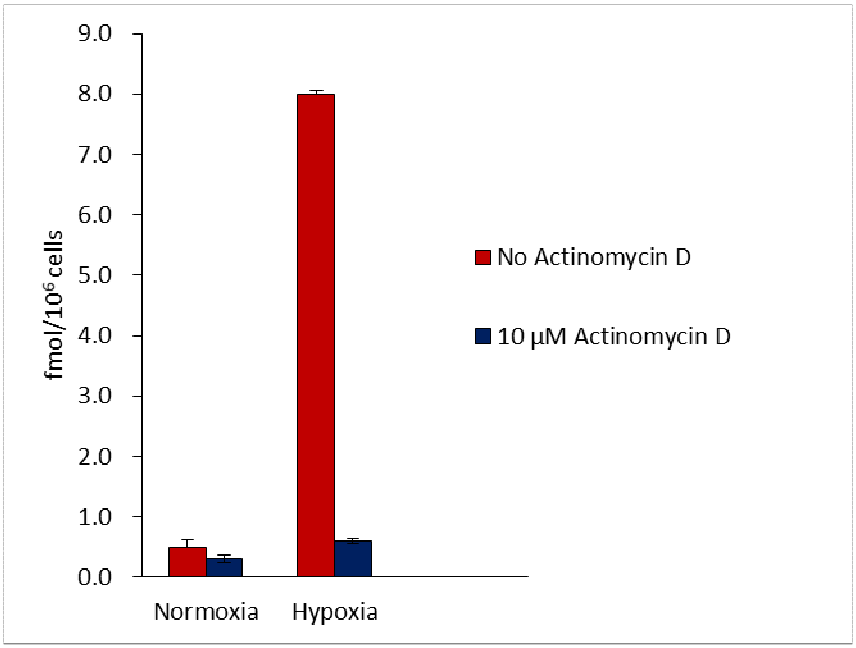

Figure 4. Binding of 2NIHC to HeLa cells.

2NIHC was incubated with hypoxic or normoxic HeLa cells in the presence or absence of 10 μM Actinomycin D.

3.3 Computational Analysis

2.3.1 Linear Interaction Energy Model

RSC Advances Accepted Manuscript

Molecular modeling is a key tool in drug designing to predict the predominant binding modes of a ligand with protein of known three-dimensional structures. There are two aims of docking studies: accurate structural modeling and correct prediction of activity. The choice of best docked structure is made using a model energy score. Thus linear interaction energy (LIE) approach has been used to evaluate the binding free energy of this class of CK2α inhibitors. Several important structural features like glide score, glide energy, interaction energy of H-bond, coulomb and vander walls energy score of coumarin derivatives (Figure 5) are identified from a qualitative analysis of their activity on CK2α (Table II). The ranking of ligands is based on glide score. As summarized in Table II 2NIHC proved totally refractory to all compounds with higher glide score of -9.5 against protein kinase CK2α. It means, it can fit well in the receptor cavity and forming energetically most stable drug receptor complex. More the glide score, higher the inhibitory activity of ligand to proliferating tumor.

Primarily hydroxyl group at the 7 position of coumarin moiety is considered as essential feature to increase the inhibitory potency. Analysis of the lipophilic contact term (-4.4) clearly reveals that the binding site is very hydrophilic and hydrophilic interactions dominate (Table II). The vander Waals energy is considered to be the main energy term favoring binding. Even with less favorable van der Waals energy for 10 (-40.1 kcal/mol) in comparison to 11 i.e. -50.6 kcal/mol, ligand 4NIHC achieves the highest glide score. The E_{model} energy term of -75.1kcal/mol for the highest ranked ligand 10 shows that this is the dominant interaction controlling the ranking of a ligand. For instance, in 4NIHC substitution of nitro group at position 2 results in loss of activity with glide score decrease from -9.5 to -3.6. Altough the EvdW and Ecoul energy terms for 11 is higher

RSC Advances Accepted Manuscript

than 10 but possess low glide score due to low Emodel and Hbond values. However the contribution of Hbond for 10 is -2.1 which is highest among the other coumarin derivatives and revealed that there is good hydrogen bonding interation between ligand 10 and the crystal structure of protein complex CK2α.

3.3.2 Ligand-Receptor Docking

2NIHC was analysed in the CK2α binding pocket, which provide not only the relationship between the molecular structure and their activity but also provide the valuable clues for drug designing. As determined from the LIE model that 4NIHC possess the highest glide score, so it is docked with CK2α. The CK2α inhibitor is small and largely planar, which makes it feasible to lay out the nearby residues in a manner that is qualitatively representative of the actual 3D environment. A total of 19 residues in proximity of ligand along with hydrogen bonding interaction are shown in Figure 5. The ligand is anchored into the active site by four hydrogen bonds, including a donor and an acceptor interaction with the sidechain of Glu114 and Val116 and a donor interaction with backbone of Asp175 and Asn161 shown by purple arrows. Imidazole ring oriented parallel to protein structure for a possible π-π interaction with the His160. Apart from an imidazole ring at one end of the ligand which projects out slightly from the active site, the ligand fit well within the cavity, which is shown by the continuity of the substitution contour line. Most of the ligand is deeply buried and shows a negligible solvent exposure, except for the exposed corner of imidazole ring.

RSC Advances Accepted Manuscript

Table II. Molecular docking results of 2NIHC, 4NIHC compared with well known anticancer coumarin derivative against crystal structure of protein kinase CK2α [PDB ID: 2ZJW].

Compound	G* Score	EvdW	Ecoul	Emodel	Glide Hbond	Lipo
10	-9.5	-40.1	-19.4	-75.5	-2.1	-4.4
11	-3.6	-46.6	-41.4	-58.1	-1.4	-2.7
Reference 1[24]	-7.3	-38.5	-5.6	-67.1	-1.0	-4.1
Reference 2[25]	-6.6	-50.6	-8.9	-38.5	-1.3	-3.5

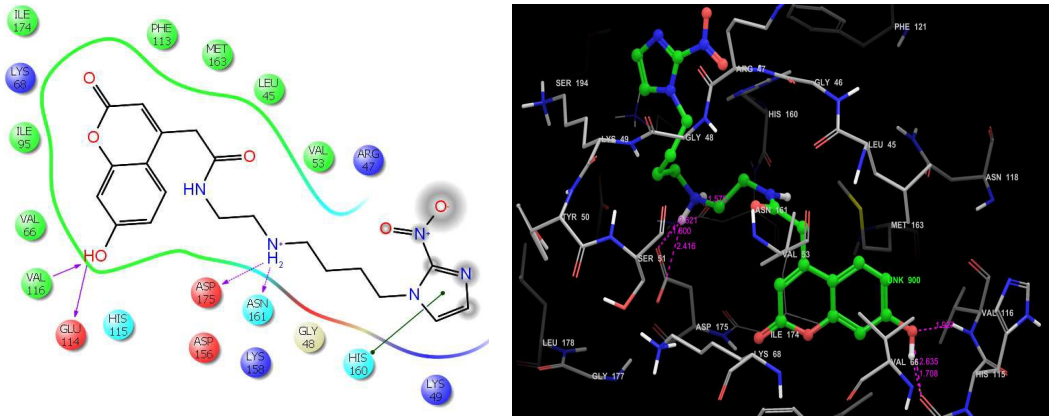

2D Placement 3D Active site

Figure 5. 2D interaction diagram of Cocrystal structure of CK2α (PDB code) with 10 hydrogen bonds with side chains of Val 116 and Glu 114, to the backbone of Asp 175 and Asn 161, by purple arrows and interaction of imidazole group with His 160 by green stick.

3.4 Radiochemistry

3.4.1 Quality control of labeled conjugate

RSC Advances Accepted Manuscript

The labeled complex remained at the origin while $^{99m}TcO_4^-$ moved toward the solvent front in acetone with R_f=1.0. The optimum pH concentration for radiolabeling was 6.0 - 7.5 and labeling efficiency for ^{99m}Tc-DO3A-BT was calculated to be >99%. *In vitro* stability of ^{99m}Tc-DO3A-BT in PBS buffer at pH 7.0 was checked at different time intervals: 4, 6, 24 and 48 h and percentage labeling efficiency at 48 h was found to be 98%, implying that labeled conjugate was stable up to 48h post labeling.

3.5 In-vivo study

3.5.1 Biodistribution study in mice bearing hypoxic tumor

In order to assess the potentiality of our approach for the design of potential radiopharmaceuticals for nuclear oncology, evaluation in mice bearing hypoxic tumor was performed. In vivo biodistribution studies of ^{99m}Tc-2NIHC and ^{99m}Tc-4NIHC were performed in BALB/c mice xenografted in their right leg with EAT tumors. The time course tissue uptake of ^{99m}Tc-2NIHC at 1, 4 and 24 h was investigated and compared with ^{99m}Tc-4NIHC at 4 h after tracer injection, where maximum uptake takes place. Results obtained at 4 h post injection (p.i). are summarized in Table III and IV.Clearance from background tissues at 1h and 4 h through blood (4.89%ID/g and 1.39%ID/g) and muscle (0.32%ID/g and 0.23%ID/g) was seems to be more rapid, so that tumor/muscle ratio of ^{99m}Tc-2NIHC increased with time and peak uptake value of 3.57(%ID/g) was observed at 4 h while for ^{99m}Tc-4NIHC it was 2.05(%ID/g) at 1h p.i. The ^{99m}Tc-2NIHC was delivered to the tumor more efficiently as compared to ^{99m}Tc-4NIHC with significant washout over time i.e. 0.24%ID/g was remained after 24 h. In general, hydrophilic character of both radioconjugates increases its clearance via renal−urinary pathway, which is preferable for the rapid clearance of background signals in images. Their kidney

RSC Advances Accepted Manuscript

uptakes were high i.e. 22.41±1.04%ID/g at 1 h for ^{99m}Tc-4NIHC and 37.99±%ID/g at 4 h for ^{99m}Tc-4NIHC indicative of extensive metabolism in the kidney. High uptake values of ^{99m}Tc-4NIHC and ^{99m}Tc-2NIHC in liver (15.53±1.04% and 13.27±1.04%) indicates that they are eliminated from the body via renal as well as by hepatobiliary pathways. No significant uptake in stomach suggests the in vivo stability of both compounds.

Table III. Biodistribution of ^{99m}Tc-4NIHC in BALB/c mice bearing EAT hypoxic tumor at 4 h p.i.[a]

Organ	%ID/g		
	1h	4 h	24h
Blood	4.82±0.12	2.67±0.14	2.75±0.07
Heart	1.88±0.2	0.83±0.11	0.82±0.08
kidney	22.41±1.04	18.37±1.09	12.60±0.95
Liver	15.53±1.04	11.21±0.68	10.05±0.22
Lungs	1.65±0.14	1.78±0.21	2.89±0.08
Stomach	0.97±0.14	0.89±0.12	0.75±0.08
Muscle	0.81±0.02	0.44±0.01	0.45±0.002
Tumor	1.66±0.02	0.86±0.01	0.32±0.02
T/M ratio	2.05±0.34	1.99±0.27	1.02±0.29

[a] Values are expressed as the mean ± SD; n = 3.

RSC Advances Accepted Manuscript

Table IV. Biodistribution of ^{99m}Tc-2NIHC in BALB/c mice bearing EAT hypoxic tumor at 4 h p.i.[a]

Organ	%ID/g		
	1h	4 h	24h
Blood	4.89±0.12	1.39±0.14	0.24±0.07
Heart	0.55±0.2	1.35±0.11	0.13±0.08
kidney	29.60±1.04	37.99±1.09	17.73±0.95
Liver	13.27±1.04	9.05±0.68	1.47±0.22
Lungs	9.23±0.14	5.69±0.21	2.46±0.08
Stomach	0.85±0.14	0.52±0.12	0.18±0.08
Muscle	0.32±0.02	0.23±0.01	0.07±0.002
Tumor	0.59±0.02	0.83±0.01	0.20±0.02
T/M ratio	1.82±0.34	3.57±0.27	2.97±0.29

[a]Values are expressed as the mean ± SD; n = 3.

3.5.2 Scintigraphy in mice bearing normal and hypoxic tumor

Based on literature reports the effect of hypoxia on drug sensitivity had suggested that there was consistently more cytotoxicity under hypoxic conditions for the drugs. Both the ligands were studied for scintigraphic imaging at 1 h p.i shown in Figure 6. The 1 h p.i. whole body planar image of the unblocked mouse demonstrated increase uptake in the tumor sites as well as in kidneys, liver, intestine and bladder in descending level of intensity relative to the background soft tissues. Tumor grafted in BALB/c mice clearly identifiable in the γ camera images (Fig. 6a) and showed high target to non target ratio of ^{99m}Tc-2NIHC. Blocking study was also performed which confirmed the selectivity of

RSC Advances Accepted Manuscript

these radioligands. Due to high abdominal uptake, as seen with ^{99m}Tc-2NIHC, the potential application of radiotracers could be envisaged for imaging primary tumors that are outside the abdomen.

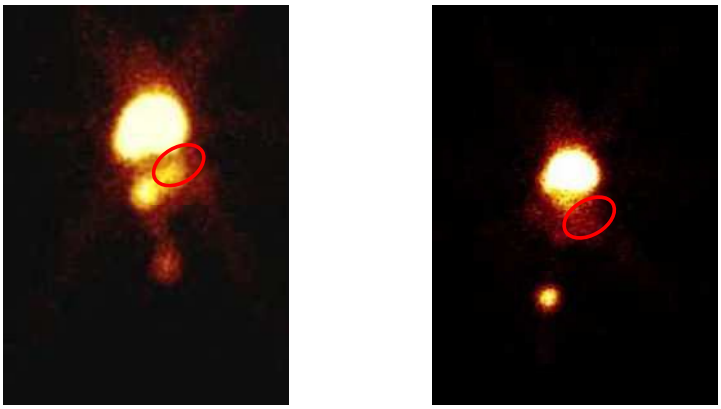

^{99m}Tc-4NIHC ^{99m}Tc-2NIHC

[A]

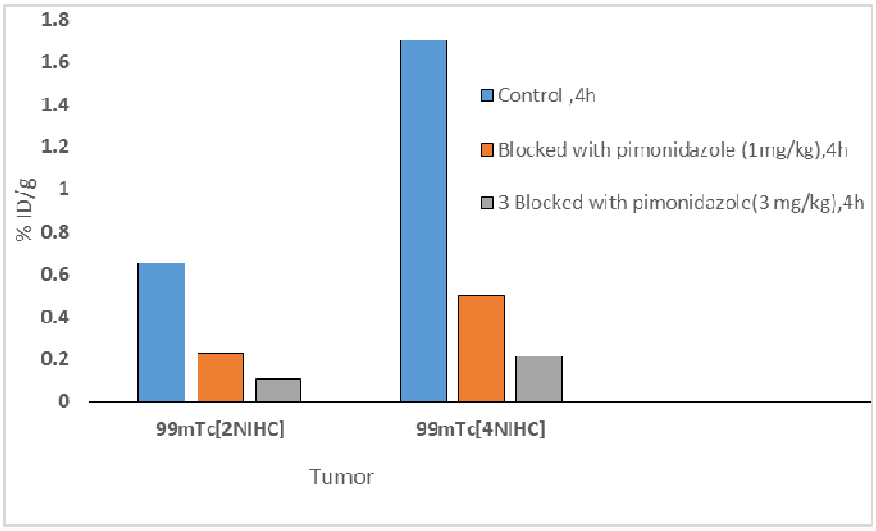

[B]

Figure 6. Whole-body γ image of BALB/c mice with tumor in right thigh (red circle indicate tumor site) at 1 h p.i. (A) Effect of blocking studies with pimonidazole (B)

RSC Advances Accepted Manuscript

3.5.3 Antitumor Screening

In vivo animal studies were carried out to examine targeting and antitumor effects of 2NIHC using an EAT bearing BALB/c mice model. The growth of tumor volume was observed for 30 days after treatment with 2NIHC and control group which was without any vehicle at two dose rate 5mg/kg and 30 mg/kg body weight (Figure 7). 2NIHC dominantly controlled tumor growth compared to control group as demonstrated by calculating tumor volume (mm^3), thus constitute it as an interesting candidate for the development of conceptually novel anticancer drug. The inhibitor concentrations were well tolerated and there was no significant reduction in weight of any of the mice during the tumor regression study. The result indicated that 2NIHC reduced the tumor growth as compared to control mainly at dose of 30 mg/kg and increased the survival time, constituting it as interesting candidates for the development of anticancer drugs.

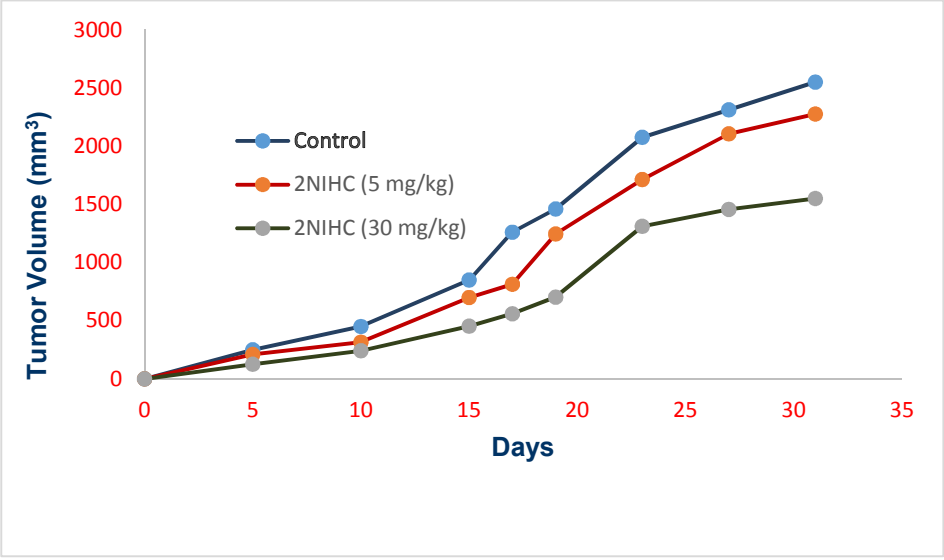

Figure 7. Tumor growth inhibition in EAT-bearing BALB/c mice

Data represented are mean of three animals experiment. 2NIHC was given at a dose of 5mg/kg and 30 mg/kg on 15th, 17th, 19th and on 23rd day. Control was considered without any vehicle.

RSC Advances Accepted Manuscript

4. Conclusion

In conclusion, we have synthesized and evaluated two nitroimidazole conjugated fluorophore systems, 2NIHC and 4NIHC for the purpose of enhancing retention in hypoxic cells. Computational docking study showed that the 2NIHC is potent CK2 inhibitor. The flow cytometry demonstrated that only 2NIHC showed improved retention in hypoxic relative to normoxic cells. *In vitro* studies confirm its potential and selectivity for hypoxic cells. Further logitunal animal studies and optimization may give a lead for new small molecule based agent which may be useful for clinical application.

Acknowledgments

We are highly thankful to Dr R. P. Tripathi, Director INMAS, for providing necessary facilities. The work was supported by Council of Scientific and Industrial research (CSIR) and Defence Research and Development Organization, under R&D project INM-311(3.1).

This is also certified that there is no interest of conflict between the authors of this manuscript.

References

RSC Advances Accepted Manuscript

1. Zhou J, Schmid T, Schnitze S, Brune B. Cancer hypoxia and cancer progression. Cancer Letters.2006; 237(1):10-21.

2. Vaupel P, Harrison L. Tumor hypoxia: causative factors, compensatory mechanisms and cellular response. Oncologist.2004; 9(5): 4-9.

3. Browm JM. Tumor hypoxia in cancer therapy. Methods Enzymol.2007; 435(10): 297-321.

4. Shannon, AM, Bouchier-Hates, DJ, Condron, CM, Toomey D. Tumor hypoxia, chemotherapeutic resistance and hypoxia related therapies. Cancer Treat. Rev.2003; 29(4):297-307.

5. Lyng H, Sundfor K, Rofstad EK. Oxygen tension in human tumors measured with polarographic needle electrodes and its relationship to vascular density, necrosis and hypoxia. Radiotherm. Oncol.1997; 44(2):163-169.

6. Nunn A, Linder K, Strauss HW. Nitroimidazoles and imaging hypoxia. Eur. J. Nucl. Med. Mol. Imaging. 1995;22(3): 265-280.

7. Mees G, Diercks R, Vangestel C, Wiele CV. Molecular imaging of hypoxia with radiolabeled agents. Eur. J. Nucl. Med. Mol. Imaging. 2009; 36(10): 1674-1886.

8. Ziemer LS, Evans SM, Kachur AV, Shuman AL, Cardi CA, Jenkins WT, Karp J S, Alavi A, Dolbier WR, Koch CJ. Non invasive imaging of hypoxia in rats using the 2-nitroimidazole ^{18}F-EF5. Eur. J. Nucl. Med. Mol. Imaging.2003; 30(2): 259-266.

9. Kaisa L, Vesa O, Samuel N, Tove G, Anne R, Olli E, Heikki M. Quantifying tumor hypoxia with ^{18}F-Fluroerythronitroimidazole (^{18}F-FETNM) using tumor to plasma ratio. Eur. J. Nucl. Med. 2003;30(3): 101-108.

RSC Advances Accepted Manuscript

10. Linder KE, Chan YW, Cyr JE, Malley MF, Nowotnik DP, Nunn AD. TcO(PnAO-1-(2-nitroimidazole)) [BMS-181321], a new technetium-containing nitroimidazole complex for imaging hypoxia: synthesis, characterization, and xanthine oxidase-catalyzed reduction J. Med. Chem. 1994;37(1) :9-17.
11. Melo T, Duncan J, Ballinger JR, Rauth AM. BRU59-21, a second generation ^{99m}Tc-Labeled 2-Nitroimidazole for Imaging Hypoxia in tumors. J. Nucl. Med.2000; 41(1): 169-176.
12. Wang SJ, Lo JM, Shen LH, Wey SP. Tumor Uptake of ^{99m}Tc-HL91 and ^{99m}Tc-PnAO-Nitroimidazole in an Animal Model of Non-small Cell Lung Cancer. Ann. Nucl. Med. Sci.2004; 17:139-146.
13. Okada RD, Johnson G, Nguyen KN, Edwards B, Archer CM, Kelly JD. 99mTc-HL91 effects of low flow and hypoxia on a new ischemia-avid myocardial imaging agent. Circulation, 1997; 95: 1892-1899.
14. Cook GJR, Houston S, Barrington SF, Fogelman I. Technetium-99m-labeled HL91 to identify tumor hypoxia: correlation with fluorine-18-FDG. J. Nucl. Med.1998; 39: 99-103.
15. Wardman P, Clarke ED, Hodgkiss RJ, Middleton RW, Parrick J, Stratford MRL. Nitroaryl compounds as potential fluorescent probes for hypoxia. II. Identification and properties of reductive metabolites. Int. J. Radiat. Oncol. Biol. Phys. 1984;10(8): 1353-1356.
16. Hodgkiss RJ, Jones GW, Long A, Middleton RW, Parrick J, Stratford MRL, Wardman R, Wilson GD. Fluorescent markers for hypoxic cells: a study of

RSC Advances Accepted Manuscript

nitroaromatic compounds, with fluorescent heterocyclic side chains, that undergo bioreductive binding. J. Med. Chem. 1991;34(7) :2268-2274.

17. Zhu Q, Uttamchandani M, Li D, Lesaicherre ML, Yao SQ. Enzymatic profiling system in a small molecule array. Org. Lett. 2003;5(8): 1257-1260.
18. Kostova I. Synthetic and natural coumarins as cytotoxic agents. Curr. Med. Chem. Anticancer Agents.2005; 5(1): 29-46.
19. Dan Z, Jennifer H, Robert H, Mahan A, Owen P, Gordafaried D, Xueqyn HH, Sarah C. Inhibition of protein Kinase CK2 expression and activity blocks tumor growth. Mol. Cell. Biochem.2010; 333(4): 159-167.
20. Adriana C, Roberto B, Andrea B, Giorgio C, Samuele Z, Giorgia P, Marco M, Giuseppe Z, Eugenio U, Adriano G, Lorenzo AP, Flavio M. and Stefano M. Coumarin as Attractive Casein Kinase 2 (CK2) Inhibitor Scaffold: An Integrate Approach to elucidate the Putative Binding Motif and Explain Structure–Activity Relationships. J. Med. Chem.2008; 51(4): 752-759.
21. Wang T, Nik T, Goto A, Ota S, Morikawa T, Nakamura Y, Ohara E, Ishikawa S, Aburatani H, Nakajima J, Fukayama M. Hypoxia increases the motility of lung adenocarcinoma cell line A549 via activation of the epidermal growth factor receptor pathway. Cancer Science, 2007;98: 506-518.
22. Schnitzer SE, Schmid T, Zhou J, Brüne B. Hypoxia and HIF-1protect A549 cells from drug-induced apoptosis. Cell Death and Differentiation. 2006; 13: 1611-1613.
23. Wagh NK, Zhou Z, Ogbomo SM, Shi W, Brusnahan SK, Garrison JC. Development of hypoxia enhanced ^{111}In-labeled bombesin conjugates: Design,

RSC Advances Accepted Manuscript

Synthesis and In Vitro evaluation in PC-3 human prostate cancer. Bioconjugate Chemistry,2012; 23:527-537.

24. Nadia T, Alfonso M, Paul CM, Yuanmei L, Andrea S, Shoukat D, Jean-Yves W, and Claudiu TS. Glycosyl Coumarin Carbonic Anhydrase IX and XII Inhibitors Strongly Attenuate the growth of primary breast tumor. J. Med. Chem.2011; 54(24): 8271-8277.
25. Koneni VS, Abdhesh K, Manoj K, Jayanta S, Sudhir S. Synthesis and in vitro evaluation of novel coumarin–chalcone hybrids as potential anticancer agents. Biorg & Med Chem Letters, 2010;20(24): 7205-7211.

RSC Advances Accepted Manuscript